NANO LETTERS
Cite This: Nano Lett. 2019, 19, 1701−1705
Letter
pubs.acs.org/NanoLett

Engineered Mesenchymal Stem Cell/Nanomedicine Spheroid as an Active Drug Delivery Platform for Combinational Glioblastoma Therapy

Smruthi Suryaprakash,[†,¶] Yeh-Hsing Lao,[†,¶] Hyeon-Yeol Cho,[‡,¶] Mingqiang Li,[†] Ha Yeun Ji,[†] Dan Shao,[†] Hanze Hu,[†] Chai Hoon Quek,[†] Dantong Huang,[†] Rachel L. Mintz,[†] Juli R. Bagó,[§] Shawn D. Hingtgen,[§] Ki-Bum Lee,[‡] and Kam W. Leong*[,†,⊥]

[†]Department of Biomedical Engineering, Columbia University, New York, New York 10027, United States
[‡]Department of Chemistry and Chemical Biology, Rutgers, The State University of New Jersey, Piscataway, New Jersey 08854, United States
[§]Division of Molecular Pharmaceutics, UNC Eshelman School of Pharmacy, University of North Carolina at Chapel Hill, Chapel Hill, North Carolina 27599, United States
[⊥]Department of Systems Biology, Columbia University Medical Center, New York, New York 10032, United States

Supporting Information

ABSTRACT: Mesenchymal stem cell (MSC) has been increasingly applied to cancer therapy because of its tumor-tropic capability. However, short retention at target tissue and limited payload option hinder the progress of MSC-based cancer therapy. Herein, we proposed a hybrid spheroid/nanomedicine system, comprising MSC spheroid entrapping drug-loaded nanocomposite, to address these limitations. Spheroid formulation enhanced MSC's tumor tropism and facilitated loading of different types of therapeutic payloads. This system acted as an active drug delivery platform seeking and specifically targeting glioblastoma cells. It enabled effective delivery of combinational protein and chemotherapeutic drugs by engineered MSC and nanocomposite, respectively. In an *in vivo* migration model, the hybrid spheroid showed higher nanocomposite retention in the tumor tissue compared with the single MSC approach, leading to enhanced tumor inhibition in a heterotopic glioblastoma murine model. Taken together, this system integrates the merits of cell- and nanoparticle- mediated drug delivery with the tumor-homing characteristics of MSC to advance targeted combinational cancer therapy.

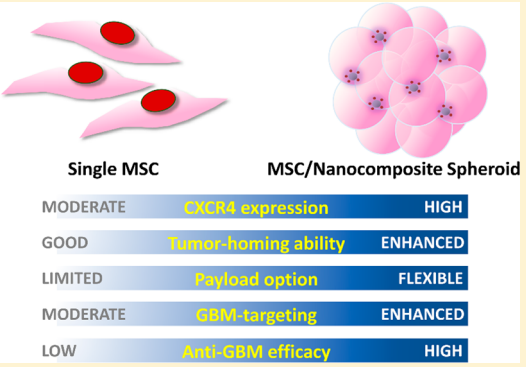

KEYWORDS: *Mesenchymal stem cell, nanomedicine, glioblastoma, targeted therapy, cell spheroid*

Certain types of stem cells, including mesenchymal stem cell (MSC), neural stem cell, and hematopoietic stem cell, show tumor-homing capability. They pursue the chemotaxis gradient, such as C-X-C motif chemokine 12, generated by cancer cells.[1,2] With genetic modification, engineered stem cells could act as drug carriers homing to tumor and repressing tumor growth via the secretion of cytotoxic proteins.[3] Especially for glioblastoma (GBM), preclinical studies have shown that treating GBM-bearing animals with engineered stem cells improves the therapeutic outcome. The phase I clinical trials, administering stem cells at the resection cavity after tumor removal, confirm the safety of this therapeutic strategy.[4,5]

However, cell retention is a major obstacle limiting the efficacy of engineered stem cell-based therapy. For example, a recent study in the preclinical mouse GBM model showed that >90% of the stem cells that were locally administered at the tumor resection site were lost within 7 days, and rapid GBM relapse was consequently observed.[6] Limited payload option is another obstacle. Transduced stem cells can only biosynthesize protein- and peptide-based drugs, which may not be sufficient to treat GBM. For example, the tumor necrosis factor-related apoptosis-inducing ligand (TRAIL), a protein drug that can initiate the formation of death-inducing signaling complex via the interaction with its receptors and subsequently induces cell apoptosis, is used to treat GBM in clinical trials and the preclinical pipeline.[7,8] However, it showed limited efficacy for treating certain types of the GBM cells such as U87MG and LN229 (Figure S1A, Supporting Information).

A combinational approach with another small-molecule drug may improve the therapeutic efficacy. A previously published study found that mitoxantrone (MTX) could sensitize the

Received: November 21, 2018
Revised: February 11, 2019
Published: February 18, 2019

DOI: 10.1021/acs.nanolett.8b04697
Nano Lett. 2019, 19, 1701−1705

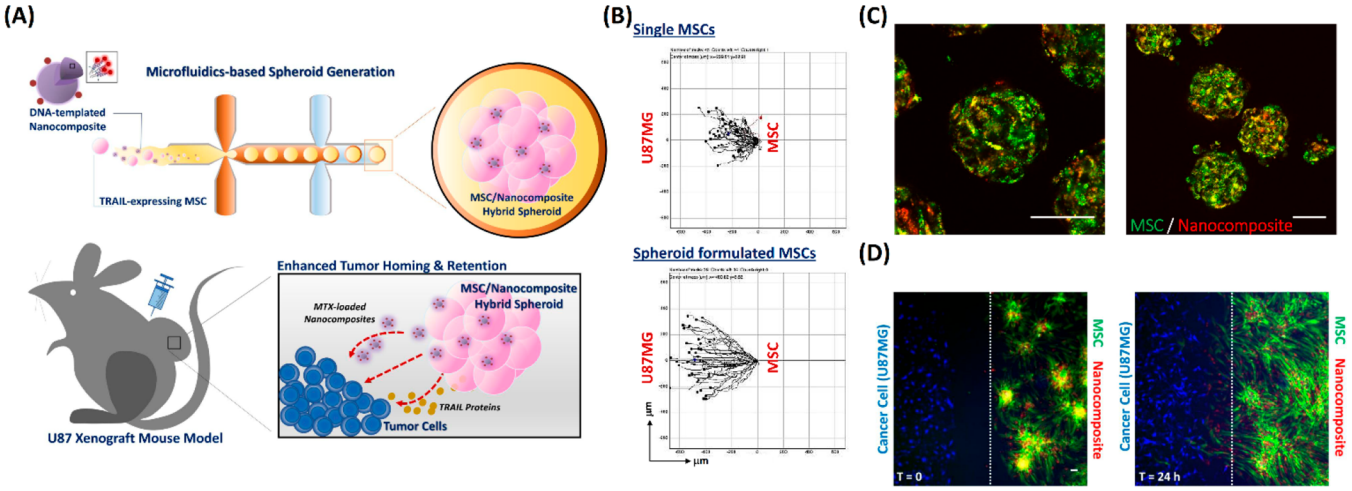

Figure 1. Design and properties of MSC/DNA-templated nanocomposite hybrid spheroid for GBM therapy. (A) Schematic illustration of the hybrid spheroid system. (B) Comparison of the *in vitro* tumor homing property between single and spheroid-formulated MSCs. (C) Representative confocal images of the hybrid spheroids. (D) *In vitro* tumor homing of the hybrid spheroids. Scale bar = 50 μm.

response of TRAIL in the GBM cell lines.[9] On one hand, we found that cotreating the GBM cells (U87MG, LN229, T98G, and LN18) with both TRAIL and MTX could enhance the efficacy *in vitro*, resulting in more than one order-of-magnitude improvement of the IC50s (Figure S1B, Supporting Information). However, the lack of an efficient delivery method for both TRAIL and MTX is an issue. Although some works have demonstrated the possibility of loading MSC with other types of drugs and targeted drug release through MSC's endocytosis/exocytosis[10−12] or using a surface modification approach,[13,14] the efficiency of these delivery approaches is still a concern. For example, for the endocytosis/exocytosis approach, the payload's characteristics (size, charge, and shape) would affect its loading and release.[15] On the other hand, the surface modification approach may need special engineering on MSC cell membrane.[2] To tackle these issues, we instead propose a hybrid MSC/nanomedicine spheroid system, which incorporates TRAIL-engineered MSC and MTX-loaded nanocomposite, for enhanced cancer therapy (Figure 1A).

To generate the hybrid MSC/nanomedicine spheroid, we chose the microfluidics-based approach that has been reported to enable more uniform and faster spheroid generation over other approaches by us and other groups.[16−19] Following our previously published microfluidics method,[19] we first optimized the cell input density for the spheroid generation. Similar to what was observed in the other study,[17] the spheroid size was a function of the input density, and it reached ∼150 μm in diameter when the input density was increased to 3×10^7 cells/mL (Figure S2A, Supporting Information). Yet, increasing the input density to 3×10^7 cells/mL compromised MSC's viability (Figure S2B, Supporting Information), only reaching 80% of that with lower densities ($p < 0.01$), so we chose the two lower densities for the following experiments. Next, we verified whether the spheroid formation could enhance MSC's tumor homing property. As shown in Figure 1B, on an *in vitro* migration assay chamber with a ∼500 μm gap between the MSC and U87MG cells, spheroid-formulated MSCs migrated toward the U87MG side at a faster rate compared with the single MSCs. Quantitatively, the spheroid formulation improved by 1.5−2-fold in speed as well as distance in this *in vitro* migration assay (Figure S3, Supporting Information). We attribute this finding to the boost in MSC's chemotaxis sensing receptor, C-X-C chemokine receptor type 4 (CXCR4), expression in the spheroid.[20−22] The increase in CXCR4 expression level was a function of the MSC input density in the microfluidic spheroid formation, reaching six-times higher than that in the single MSC when the input density was 2×10^7 cells/mL (Figure S4, Supporting Information). When the MSC cell was treated with the CXCR4 antagonist, AMD3100,[23] its migration toward the U87MG was inhibited, confirming the role of CXCR4 in MSC's tumor homing property (Figure S5, Supporting Information).[24,25] In addition, this MSC migration was driven by the chemotaxis established by the cancer cells, as the MSCs would move in a typical random walk motion when the U87MG was not present (Figure S6, Supporting Information).

Although the spheroid formulation boosted the migration rate and distance, it did not improve the TRAIL protein expression nor enhance the efficacy *in vitro* (Figure S7, Supporting Information). These results again supported the argument that combinational therapy would be essential to improve the therapeutic efficacy against GBM. To do so, we introduced a DNA-templated nanocomposite system for MTX delivery. The DNA template is a PEGylated DNA, and it forms nanocomposite via the calcium phosphate (CaP) nanoprecipitation.[26,27] Specifically, the nanocomposite forms through the interaction between the phosphate backbone of the template and the Ca^{2+} ions in the solution; the PEG component confines the precipitation. The nanocomposite generated by this method is therefore both size-controllable and uniform. Without PEG, the generated nanocomposite aggregated immediately after it was mixed with Ca^{2+}-containing buffer. In contrast, the PEGylation enabled nanosized, monodispersed nanoparticle generation (Figure S8A, Supporting Information). Zhang et al. demonstrated that longer PEG offered stronger steric repulsion, which benefited the colloidal stability, and the DNA-templated nanocomposite generated with 12−15 kDa of PEG was more stable, compared with the one with shorter PEG (<5 kDa).[28] Motivated by this observation and the goal to prevent undesired MSC uptake, we tested the combinations of two PEGs (10 or 20 kDa) and two DNA lengths (20 or 40 mer). Compared with the shorter PEG, the longer PEG (20 kDa) did not dramatically increase the

DOI: 10.1021/acs.nanolett.8b04697
Nano Lett. 2019, 19, 1701−1705

nanocomposite size, but it enhanced the nanocomposite stability when combined with the longer DNA (Figure S8B, Supporting Information). As a result, we chose both the longer PEG and DNA for better drug loading in the following experiments. For the drug loading, MTX and other drugs in the anthracenedione family could be easily loaded into the nanocomposite through intercalation.[29] The intercalation-based interaction has been widely used in different applications such as biomolecule tracking,[30,31] biosensing,[32,33] and drug delivery.[34−37] To test if this interaction could give us better loading, we used the fluorescent drug that holds similar DNA recognition preference, bisantrene,[29] as a model compound to verify our system's loading efficiency and level. The loading efficiency reached nearly 100% when the template/drug ratio was close to 10, whereas the maximum loading level (∼20%) was observed when the ratio was 0.02 (Figure S8C, Supporting Information). Compared with the previously reported MTX delivery systems, the loading level of our nanocomposite system was 2.5−7-times higher.[38,39] Other than enhanced drug loading, the DNA nanostructure-based delivery systems[34,35] act like other types of nanoparticle, releasing the drugs when under the acidic microenvironment of the endosome,[37] but notably, DNA nanostructures could tune the acidity of endosomal/lysosomal compartments to circumvent the drug resistance mechanism induced by the cancer cells.[36]

In the presence of the DNA-templated nanocomposites, MSCs could form spheroids (Figure 1C) using the microfluidics technique without losing the tumor-homing property and affecting the viability of MSCs (Figure 1D, Figure S9, and Supplementary Video 1, Supporting Information). We then investigated the distribution of the nanocomposites in the spheroid using a dual-labeling approach. The PEG and DNA segments were first labeled with Alexa Flour 647 and Fluorescein (FAM), respectively. After forming a nanocomposite, the green fluorescence was quenched due to the self-quenching effect of FAM in the CaP core. If the nanocomposite was internalized by the MSC, the green fluorescence would light on again, as the nanocomposite disassembled (Figure S10A, Supporting Information). By checking the Alexa Flour 647 and FAM signals, we verified the nanocomposite location after the spheroid formation. In 2D monolayer culture, as expected, most of the nanocomposites were only associated with the MSCs but not internalized. In 3D spheroidal culture, we observed increased uptake, but a significant portion of the nanocomposites were still intact and probably located in the extracellular matrix part of the spheroid (Figure S10B, Supporting Information).

We next investigated if this design could efficiently and specifically kill GBM cells; we used the TRAIL-secreting MSC (TRAIL-MSC) and MTX-loaded nanocomposite to generate the hybrid spheroid. To further enhance the targeting capability, we decorated our nanocomposite with a peptide ligand[40] against IL13Rα2, a surface marker for certain types of GBM cells.[41,42] After testing a panel of the GBM cells, we chose three GBM cells with high to low IL13Rα2 expression (U87MG, GBM8, and LN18; Figure S11A, Supporting Information) for the *in vitro* validation. When the high IL13Rα2-expressing U87MG cells were treated with ligand-decorated nanocomposites, the cells could efficiently internalize the nanocomposites (Figure S11B, Supporting Information), which resulted in a significant improvement in the cell-kill efficacy against U87MG cells compared with the group either treated with TRAIL-MSC spheroids or free MTX-loaded, TRAIL-MSC spheroids (cancer cell's viability dropped from 68% to 34%, $p < 0.001$; Figure 2). The improvement

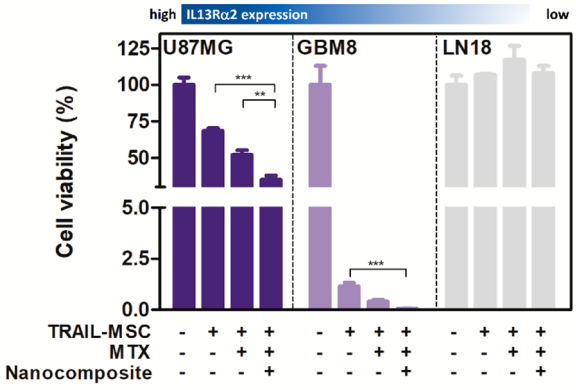

Figure 2. *In vitro* GBM cell kill evaluation. The cancer cells were treated with TRAIL-MSC spheroids, free MTX-loaded TRAIL-MSC spheroids, or the TRAIL-MSC/MTX-loaded nanocomposite hybrid spheroids. Data are represented as average ± standard error of mean (SEM; $n = 4$). Statistical analysis was done using one-way ANOVA with Tukey post hoc test, and the significance was represented as ** ($p < 0.01$), *** ($p < 0.001$).

could be also observed in the other IL13Rα2-expressing cell type, GBM8 (1.14% to 0.41%), but not in the low IL13Rα2-expressing cell type (LN18). These results suggest the high efficacy and specificity of the hybrid spheroidal delivery system.

As aforementioned, cell retention is one of the major issues that limits the efficacy of MSC-based cell therapy. We examined if the hybrid spheroid could address this problem by providing longer retention in the tumor site *in vivo*. For this purpose, we established a heterotopic GBM model, which has been commonly used for preclinical validation[43,44] and might still conserve most of the molecular characteristics.[44,45] The mouse was first inoculated with U87MG subcutaneously. To track the migration, MSC and nanocomposite were labeled with Luciferase and Alexa Flour 680, respectively. The hybrid spheroid or the single MSC/nanocomposite mixture was given at the edge of the tumor. As shown in Figure 3A, when mice were treated with the single MSC/nanocomposite mixture, a significant amount of the injected nanocomposite was cleared within a week, although the MSC's Luciferase signal was still detected strongly. In contrast, the group given with the hybrid spheroid showed strong signals on both channels. By normalizing the signal to that on the day of administration (day 0), only 11.5% of the nanocomposite was removed 1 day after the administration for the group treated with the hybrid spheroid, while 76.5% was removed for the group treated with single MSC/nanocomposite mixture (Figure 3B). At the end point (day 22), there was still 11% of the nanocomposite retaining at the tumor site, which was nearly 100-times higher than the nanocomposite amount detected in the control group of single MSC/nanocomposite mixture.

We next evaluated if better retention could lead to better therapeutic outcome. We established the tumor model in a similar fashion. The mice were first subcutaneously inoculated with mCherry-transduced U87MG cells, and after tumor formed, they were treated with drug-carrying spheroid composed of TRAIL-MSC and MTX-loaded, targeted nanocomposite. Either hybrid spheroid or the single MSC/nanocomposite mixture was administered at the edge of the

DOI: 10.1021/acs.nanolett.8b04697
Nano Lett. 2019, 19, 1701−1705

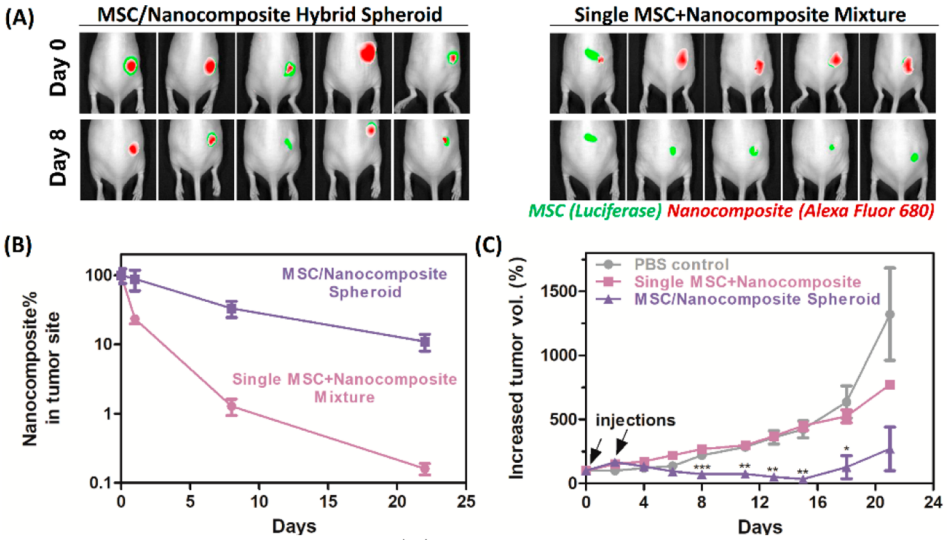

Figure 3. *In vivo* tumor homing and inhibition evaluation. (A) Representative images of the mice treated with the hybrid spheroid or single MSC/nanocomposite mixture (n = 5). (B) Nanocomposite retention in the *in vivo* migration model (n = 5). (C) Evaluation of tumor inhibition efficacy *in vivo* (n = 3). Data are represented as average ± SEM. Statistical analysis was done using one-way ANOVA with Tukey post hoc test, and the significance was represented as ∗ (p < 0.05), ∗∗ (p < 0.01), ∗∗∗ (p < 0.001).

tumor on days 0 and 2. The tumor volume was tracked for 3 weeks. The hybrid spheroid inhibited the tumor growth efficiently, but this was not the case for the group treated either with PBS or single cell/nanocomposite mixture (Figures 3C and S12A, Supporting Information). At the end point (day 21), the average tumor size of the hybrid spheroid group was 14% of that of the PBS control group, and its average tumor weight was also smaller (0.053 g vs 0.360 g; Figure S12B, Supporting Information). Also, this treatment did not show any significant toxicity in the histological analysis of the major organ sections and the spleen size measurement (Figure S12C,D, Supporting Information).

In summary, our MSC/nanomedicine hybrid spheroid strategy enables better drug retention and results in superior therapeutic outcome *in vivo*. It integrates the advantages of both cell- and nanoparticle-based therapy to deliver two different drug types with specificity for improved therapeutic efficacy.

■ ASSOCIATED CONTENT

Supporting Information

The Supporting Information is available free of charge on the ACS Publications website at DOI: 10.1021/acs.nanolett.8b04697.

Materials and methods, supplementary figures (PDF)

Supplementary video (AVI)

■ AUTHOR INFORMATION

Corresponding Author

*E-mail: kam.leong@columbia.edu. Phone: +1-212-342-3152.

ORCID

Hyeon-Yeol Cho: 0000-0003-1897-1166

Mingqiang Li: 0000-0002-5178-4138

Hanze Hu: 0000-0003-2109-1311

Kam W. Leong: 0000-0002-8133-4955

Author Contributions

¶These authors contributed equally.

Notes

The authors declare the following competing financial interest(s): A patent application related to this work has been filed (S.S., Y.-H.L., and K.W.L.).

■ ACKNOWLEDGMENTS

The authors would like to thank Dr. Hye Sung Kim, Sue Halligan, and Prof. Gordana Vunjak-Novakovic (Columbia University) for their assistance and acknowledge the technical support from Columbia Medical Center Molecular Pathology Core Facility. This work is supported partially by NIH (HL140275, AI096305, TL1TR001875) and DoD (W81XWH-12-1-0261). The human MSC used in this study was obtained from Institute for Regenerative Medicine, Texas A&M University System Health Science Center under the material transfer agreement. The animal study was approved and supervised by the Institutional Animal Care and Use Committees at Rutgers.

■ REFERENCES

(1) Aboody, K. S.; Najbauer, J.; Danks, M. K. *Gene Ther.* **2008**, *15* (10), 739−752.

(2) Park, J. S.; Suryaprakash, S.; Lao, Y. H.; Leong, K. W. *Methods* **2015**, *84*, 3−16.

(3) Sasportas, L. S.; Kasmieh, R.; Wakimoto, H.; Hingtgen, S.; van de Water, J. A. J. M.; Mohapatra, G.; Figueiredo, J. L.; Martuza, R. L.; Weissleder, R.; Shah, K. *Proc. Natl. Acad. Sci. U. S. A.* **2009**, *106* (12), 4822−4827.

(4) Aboody, K. S.; Najbauer, J.; Metz, M. Z.; D'Apuzzo, M.; Gutova, M.; Annala, A. J.; Synold, T. W.; Couture, L. A.; Blanchard, S.; Moats, R. A.; Garcia, E.; Aramburo, S.; Valenzuela, V. V.; Frank, R. T.; Barish, M. E.; Brown, C. E.; Kim, S. U.; Badie, B.; Portnow, J. *Sci. Transl. Med.* **2013**, *5* (184), 184ra59.

(5) Lesniak, M. S.; Stupp, R.; Sachdev, S.; Lukas, R.; Chandler, J.; Portnow, J.; Amidei, C.; Miska, J.; Balyasnikova, I.; Ahmed, A.; Curiel, D.; Strong, T.; LeFever, A.; Adams, A.; Giles, F.; Aboody, K. *Neuro-Oncology* **2017**, *19*, 8.

(6) Hingtgen, S. D.; Kasmieh, R.; van de Water, J.; Weissleder, R.; Shah, K. *Stem Cells* **2010**, *28* (4), 832−841.

(7) Lemke, J.; von Karstedt, S.; Zinngrebe, J.; Walczak, H. *Cell Death Differ.* **2014**, *21* (9), 1350−1364.

DOI: 10.1021/acs.nanolett.8b04697
Nano Lett. 2019, 19, 1701−1705

(8) Stuckey, D. W.; Shah, K. *Trends Mol. Med.* **2013**, *19* (11), 685−694.
(9) Senbabaoglu, F.; Cingoz, A.; Kaya, E.; Kazancioglu, S.; Lack, N. A.; Acilan, C.; Bagci-Onder, T. *Cancer Biol. Ther.* **2016**, *17* (5), 546−557.
(10) Roger, M.; Clavreul, A.; Venier-Julienne, M. C.; Passirani, C.; Sindji, L.; Schiller, P.; Montero-Menei, C.; Menei, P. *Biomaterials* **2010**, *31* (32), 8393−8401.
(11) Kang, S.; Bhang, S. H.; Hwang, S.; Yoon, J. K.; Song, J.; Jang, H. K.; Kim, S.; Kim, B. S. *ACS Nano* **2015**, *9* (10), 9678−9690.
(12) Pascucci, L.; Cocce, V.; Bonomi, A.; Ami, D.; Ceccarelli, P.; Ciusani, E.; Vigano, L.; Locatelli, A.; Sisto, F.; Doglia, S. M.; Parati, E.; Bernardo, M. E.; Muraca, M.; Alessandri, G.; Bondiolotti, G.; Pessina, A. *J. Controlled Release* **2014**, *192*, 262−270.
(13) Li, L. L.; Guan, Y. Q.; Liu, H. Y.; Hao, N. J.; Liu, T. L.; Meng, X. W.; Fu, C. H.; Li, Y. Z.; Qu, Q. L.; Zhang, Y. G.; Ji, S. Y.; Chen, L.; Chen, D.; Tang, F. Q. *ACS Nano* **2011**, *5* (9), 7462−7470.
(14) Suryaprakash, S.; Li, M. Q.; Lao, Y. H.; Wang, H. X.; Leong, K. W. *Carbon* **2018**, *129*, 863−868.
(15) Oh, N.; Park, J. H. *Int. J. Nanomed.* **2014**, *9*, 51−63.
(16) Lee, K.; Kim, C.; Yang, J. Y.; Lee, H.; Ahn, B.; Xu, L. F.; Kang, J. Y.; Oh, K. W. *Biomicrofluidics* **2012**, *6* (1), 14114−141147.
(17) Chen, K. J.; Wu, M. X.; Guo, F.; Li, P.; Chan, C. Y.; Mao, Z. M.; Li, S. X.; Ren, L. Q.; Zhang, R.; Huang, T. J. *Lab Chip* **2016**, *16* (14), 2636−2643.
(18) Siltanen, C.; Diakatou, M.; Lowen, J.; Haque, A.; Rahimian, A.; Stybayeva, G.; Revzin, A. *Acta Biomater.* **2017**, *50*, 428−436.
(19) Chan, H. F.; Zhang, Y.; Leong, K. W. *Small* **2016**, *12* (20), 2720−2730.
(20) Potapova, I. A.; Brink, P. R.; Cohen, I. S.; Doronin, S. V. *J. Biol. Chem.* **2008**, *283* (19), 13100−13107.
(21) Bartosh, T. J.; Ylostalo, J. H.; Mohammadipoor, A.; Bazhanov, N.; Coble, K.; Claypool, K.; Lee, R. H.; Choi, H.; Prockop, D. J. *Proc. Natl. Acad. Sci. U. S. A.* **2010**, *107* (31), 13724−13729.
(22) Frith, J. E.; Thomson, B.; Genever, P. G. *Tissue Eng., Part C* **2010**, *16* (4), 735−749.
(23) De Clercq, E. *Nat. Rev. Drug Discovery* **2003**, *2*, 581−587.
(24) Marquez-Curtis, L. A.; Janowska-Wieczorek, A. *BioMed Res. Int.* **2013**, *2013*, 561098.
(25) Park, S.; Jang, H.; Kim, B. S.; Hwang, C.; Jeong, G. S.; Park, Y. *PLoS One* **2017**, *12* (9), No. e0184595.
(26) Kakizawa, Y.; Kataoka, K. *Langmuir* **2002**, *18* (12), 4539−4543.
(27) Maeda, Y.; Pittella, F.; Nomoto, T.; Takemoto, H.; Nishiyama, N.; Miyata, K.; Kataoka, K. *Macromol. Rapid Commun.* **2014**, *35* (13), 1211−1215.
(28) Zhang, M. Z.; Ishii, A.; Nishiyama, N.; Matsumoto, S.; Ishii, T.; Yamasaki, Y.; Kataoka, K. *Adv. Mater.* **2009**, *21* (34), 3520−3525.
(29) Tse, W. C.; Boger, D. L. *Chem. Biol.* **2004**, *11* (12), 1607−1617.
(30) Lao, Y. H.; Li, M. Q.; Gao, M. A.; Shao, D.; Chi, C. W.; Huang, D. T.; Chakraborty, S.; Ho, T. C.; Jiang, W. Q.; Wang, H. X.; Wang, S. H.; Leong, K. W. *Adv. Sci.* **2018**, *5* (7), 1700540.
(31) Biebricher, A. S.; Heller, I.; Roijmans, R. F. H.; Hoekstra, T. P.; Peterman, E. J. G.; Wuite, G. J. L. *Nat. Commun.* **2015**, *6*, 7304.
(32) Pei, R.; Stojanovic, M. N. *Anal. Bioanal. Chem.* **2008**, *390* (4), 1093−1099.
(33) Lao, Y. H.; Chi, C. W.; Friedrich, S. M.; Peck, K.; Wang, T. H.; Leong, K. W.; Chen, L. C. *ACS Appl. Mater. Interfaces* **2016**, *8* (19), 12048−12055.
(34) Lao, Y. H.; Phua, K. K. L.; Leong, K. W. *ACS Nano* **2015**, *9* (3), 2235−2254.
(35) Linko, V.; Ora, A.; Kostiainen, M. A. *Trends Biotechnol.* **2015**, *33* (10), 586−594.
(36) Jiang, Q.; Song, C.; Nangreave, J.; Liu, X. W.; Lin, L.; Qiu, D. L.; Wang, Z. G.; Zou, G. Z.; Liang, X. J.; Yan, H.; Ding, B. Q. *J. Am. Chem. Soc.* **2012**, *134* (32), 13396−13403.
(37) Zhang, Q.; Jiang, Q.; Li, N.; Dai, L. R.; Liu, Q.; Song, L. L.; Wang, J. Y.; Li, Y. Q.; Tian, J.; Ding, B. Q.; Du, Y. *ACS Nano* **2014**, *8* (7), 6633−6643.
(38) Grund, S.; Doussineau, T.; Fischer, D.; Mohr, G. J. *J. Colloid Interface Sci.* **2012**, *365* (1), 33−40.
(39) Xu, Y. R.; Asghar, S.; Gao, S. Y.; Chen, Z. P.; Huang, L.; Yin, L. N.; Ping, Q. N.; Xiao, Y. Y. *Int. J. Nanomed.* **2017**, *12*, 7337−7350.
(40) Wang, B. Y.; Lv, L. Y.; Wang, Z. Y.; Zhao, Y.; Wu, L.; Fang, X. L.; Xu, Q. W.; Xin, H. L. *Biomaterials* **2014**, *35* (22), 5897−5907.
(41) Thaci, B.; Brown, C. E.; Binello, E.; Werbaneth, K.; Sampath, P.; Sengupta, S. *Neuro-Oncology* **2014**, *16* (10), 1304−1312.
(42) Joshi, B. H.; Plautz, G. E.; Puri, R. K. *Cancer Res.* **2000**, *60* (5), 1168−1172.
(43) Tseng, J. R.; Kang, K. W.; Dandekar, M.; Yaghoubi, S.; Lee, J. H.; Christensen, J. G.; Muir, S.; Vincent, P. W.; Michaud, N. R.; Gambhir, S. S. *J. Nucl. Med.* **2007**, *49* (1), 129−134.
(44) Huszthy, P. C.; Daphu, I.; Niclou, S. P.; Stieber, D.; Nigro, J. M.; Sakariassen, P. O.; Miletic, H.; Thorsen, F.; Bjerkvig, R. *Neuro-Oncology* **2012**, *14* (8), 979−993.
(45) Hodgson, J. G.; Yeh, R. F.; Ray, A.; Wang, N. J.; Smirnov, I.; Yu, M.; Hariono, S.; Silber, J.; Feiler, H. S.; Gray, J. W.; Spellman, P. T.; Vandenberg, S. R.; Berger, M. S.; James, C. D. *Neuro-Oncology* **2009**, *11* (5), 477−487.

DOI: 10.1021/acs.nanolett.8b04697
Nano Lett. 2019, 19, 1701−1705